



How do Microtopography Act in the Pedogenic Characteristics of Mudstone-derived Soils in Hilly Mountainous Regions?

Banglin Luo^{1†}, Jiangwen Li^{1†}, Jiahong Tang², Chaofu Wei^{1,3,4*}, Shouqin Zhong^{1,3,4*}

¹College of Resources and Environment/Key Laboratory of Eco-environment in Three Gorges Region (Ministry of Education), Southwest University, Chongqing 400715, China

²District Agro-Tech Extension and Service Center of Shapingba, Chongqing 400000, China

³Key Laboratory of Arable Land Conservation (Southwestern China), Ministry of Agriculture, Chongqing, 400715, China

⁴State Cultivation Base of Eco-agriculture for Southwest Mountainous Land, Southwest University, Chongqing, 400715, China

[†]These authors contributed equally to this work.

*Correspondence to: Shouqin Zhong (zhongsq2021@swu.edu.cn) & Chaofu Wei (weicf@swu.edu.cn)

Abstract. The topography is a critical factor that determines the characteristics of regional soil formation. Small-scale topographic changes are defined as microtopographies. As a characteristic topographic condition in hilly mountainous regions, the redistribution of water and soil materials caused by microtopography is the main factor affecting the spatial heterogeneity of soil and the utilization of land resources. In this study, the influence of microtopography on pedogenesis was investigated using soil samples formed from mudstones with lacustrine facies deposition in the middle of the Sichuan Basin and developed into hill landforms by erosion of flowing water. Soil profiles were sampled along the slopes at the summit, shoulder, backslope, footslope, and toeslope positions. The morphological, physiochemical, and geochemical attributes of profiles were analysed. The results showed that the soil thickness increased significantly with changes in the soil profile configuration from the summit to the toeslope, and the profile configuration changed from A-C to A-B-C. The migration direction of Ca and Na at the summit, backslope, and footslope changed from enrichment to leaching, whereas that of Al, Fe, and Mg changed from leaching to enrichment. At the summit and shoulder of the hillslope, weathered materials are transported away by gravity and surface erosion, and



28 new rocks are often exposed; therefore, the characteristics of soil development is relatively weak.
29 However, in flat areas such as the footslope and toeslope with sufficient water conditions, the
30 long-term contact between water, soil, and sediment leads to further chemical weathering, resulting in
31 highly developed characteristics. Microtopography can affect physicochemical properties, chemical
32 weathering, and redistribution of water and materials, resulting in differences in pedogenic
33 characteristics at different slope positions.

34 **Keywords.** Pedogenic characteristics; Physicochemical property; Mudstone; Microtopography;
35 Mineralogy

36 **1 Introduction**

37 Soil, as an independent natural body, maintains the lives and reproduction of various creatures on the
38 land surface and also develops and changes under the control of the soil-forming environment.
39 Evaluating objective and quantitative changes of soil properties caused by soil weathering and the stage
40 of soil weathering is the first prerequisite for interpreting changes in the soil environment and
41 improving the soil environment, and the soil development process behind soil resource change cannot
42 be ignored. Previously, research on topography mainly considered the effect of bioclimates caused by
43 large topography. The microtopography refers to the concept relative to the macrotopography, which
44 the amplitudes markedly smaller than the hillslope or basin scales (Thompson et al., 2010). Small-scale
45 topographic changes are defined as microtopographies (Wang et al., 2022). Microtopography strongly
46 affects energy, water, and nutrient cycling at local-site scale (Lv et al., 2023). The redistribution of
47 water and soil material caused by microtopography is the main factor in soil spatial variation and an
48 obstacle in the utilisation of soil resources (Kokulan et al., 2018), particularly in hilly mountainous
49 regions. Therefore, it is of great scientific significance to explore changes in soil weathering and
50 development under microtopographic conditions in hilly mountainous regions.

51 Pedogenesis refers to the evolution from the profile scale to the regional scale, which includes
52 significant changes in the soil under physical, chemical, or biological conditions (Leguédais et al.,
53 2016). Topography is a key factor that controls soil genesis and strongly influences the
54 physicochemical properties (Baltensweiler et al., 2020). In areas with large terrain slopes, the degree of



55 physical erosion of rocks is greater and chemical weathering is stronger (Gabet, 2007; Riebe et al.,
56 2004). Soil surface roughness and properties in different terrains and altitudes affect the development
57 of water infiltration, runoff, and drainage in different terrain parts (Vidal Vázquez et al., 2005). The
58 differences in water characteristics, coupled with strong erosion, affect the material distribution during
59 soil formation, which leads to differences in the degree of soil development in different terrain parts
60 (Darmody et al., 2005; Luo et al., 2020; Parent et al., 2008; Salako et al., 2007; Veneman et al., 1984).

61 On the scale of slopes and small watersheds, topography is the prominent factor that affects the
62 variation in soil properties, and it is also the main structural factor that controls spatial autocorrelation
63 (Wang et al., 2001). Compared to the equivalent background state without microtopography, the
64 presence of microtopography increases the proportion of rainfall infiltration (Thompson et al., 2010).
65 Within the influence of microtopography, the rainfall distribution pattern and operation mode on the
66 surface are completely different. Multiple studies have suggested that the difference in crop yield at
67 different topographic positions is mainly due to the change in soil properties caused by soil erosion
68 with topographic position (Brubaker et al., 1993; Salako et al., 2007). In addition, microtopography can
69 control a series of geomorphic processes, such as collapse, transportation, and accumulation, to change
70 the spatial redistribution of light, heat, water, and soil in a small area, thus affecting vegetation growth
71 (Baltensweiler et al., 2020; Nagamatsu et al., 2003). Moreover, microtopography can accelerate soil
72 weathering (Phillips et al., 2008). Pal et al., (2003) found that presence of microtopography resulted in
73 the development of non-alkaline and highly alkaline soils on the upper and lower slopes, respectively,
74 of the southwestern Indo-Gangetic Plain. Botschek et al., (1996) found that the organic matter content
75 was highest in the mineral topsoil on the uphill slope and decreased at the foot of the slope.

76 The mudstone-derived soils in the middle of the Sichuan Basin were mainly formed by flowing
77 water erosion. The area has predominantly hilly topography formed by flowing water erosion. Heat and
78 water are redistributed in different locations of topography, combined with severe soil erosion,
79 resulting in differences in soil particle composition, nutrient content, water holding capacity, drought
80 resistance, and fertiliser retention. Therefore, the degree of soil development is different. An effective
81 solution for soil erosion and its associated soil problems in this region is an important issue that we are
82 currently facing. The aims of the present study were (1) to explain the characteristics of soil

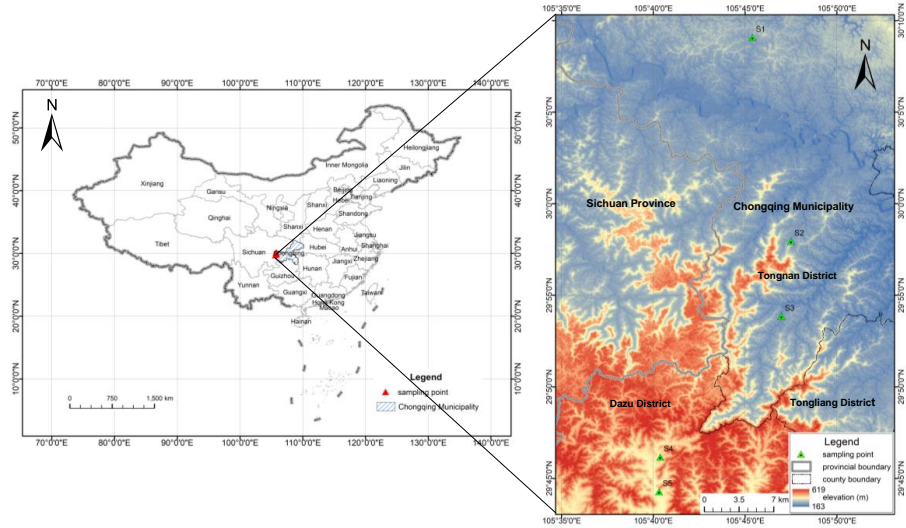


83 morphology and physiochemistry at different slope positions; (2) to explore the changes in soil
84 weathering and development under microtopographic conditions; and (3) to clarify the effect of
85 microtopography on pedogenic characteristics. Ultimately, this work provided a quantitative basis for
86 regulating the soil-forming process of mudstone soil under artificial conditions.

87 **2 Materials and methods**

88 **2.1 Study area**

89 The study area, Tongnan District and Dazu District, located in the central Sichuan Basin (Fig. 1).
90 The area has a predominantly hilly topography formed by flowing water erosion and a subtropical
91 monsoon climate. The soil samples were classified as Cambisols in the WRB classification (IUSS
92 Working Group WRB, 2022).



93
94 **Figure 1.** Study area. The background DEM dataset (30 m resolution) was downloaded from
95 Geospatial Data Cloud site, Computer Network Information Center, Chinese Academy of Sciences.
96 (<http://www.gscloud.cn>)

97 **2.2 Soil sampling**

98 Five natural and typical profiles (according to the microtopography conditions) were selected for
99 sampling (The information of sampling points was shown in Table 1). According to the 1:200,000



regional geological map of China (<https://geocloud.cgs.gov.cn>) and the field survey, the parent material of all the sampling points is purple mudstone of the Upper Jurassic Shaximiao Formation in Mesozoic. Simultaneously, in order to ensure the similarity, the other soil-forming factors such as climate (mainly rainfall and temperature) and organisms (grass and crops were the main surface vegetation, and the soil animals were shown in Table 2) besides terrain of each sampling point were also investigated (Table 1). Five soil samples with five repetitions were collected at the summit, shoulder, backslope, footslope, and toeslope positions of the hillslope (Fig. 2). Soil samples were collected from the excavated soil profile and were sampled from the toeslope to the summit according to the soil genesis characteristics (divided into horizons A, B, and C). When collecting samples, the GPS locator was used to record the coordinates, altitude, and slope of the sampling points, and the morphological characteristics of the soil profiles were recorded according to the *Field Book for Describing and Sampling Soils (version 3.0)* (Nation Soil Survey Centre et al., 2013) (Table 2). Soil samples were taken to the laboratory for chemical and physical analyses, totalling 125 samples (approximately 500 g). All the samples were air-dried. After the removal of visible plant debris, all samples were sieved through a 2 mm sieve for laboratory analysis.

Table 1. The information of sampling points.

Sampling Point	Coordinates (N/E)		Elevation (m)	Slope gradient (°)	Average annual rainfall (mm)	Average annual temperature (°C)	Land use	Slope position
S1-1	30°09'04"	105°45'31"	331	10	1121.5	18.2	Grassland	Summit
S1-2	30°09'04"	105°45'32"	320	15	1121.5	18.2	Grassland	Shoulder
S1-3	30°09'03"	105°45'18"	307	10	1121.5	18.2	Dry land	Backslope
S1-4	30°09'06"	105°45'19"	265	0	1121.5	18.2	Paddy field to dry land	Footslope
S1-5	30°09'04"	105°45'16"	242	0	1121.5	18.2	Paddy field to dry land	Toeslope
S2-1	29°57'56"	105°47'27"	330	2	1126.9	18.3	Grassland	Summit
S2-2	29°57'56"	105°47'28"	328	2	1126.9	18.3	Grassland	Shoulder
S2-3	29°57'56"	105°47'28"	314	10	1126.9	18.3	Dry land	Backslope
S2-4	29°57'58"	105°47'31"	297	10	1126.9	18.3	Dry land	Footslope
S2-5	29°57'56"	105°47'30"	265	0	1126.9	18.3	Paddy field to dry land	Toeslope
S3-1	29°53'46"	105°46'59"	319	5	1130.3	18.5	Paddy field	Summit



								to dry land	
S3-2	29°53'46"	105°46'59"	301	10	1130.3	18.5	Dry land	Shoulder	
S3-3	29°53'48"	105°47'00"	298	6	1130.3	18.5	Dry land	Backslope	
S3-4	29°53'53"	105°47'00"	267	0	1130.3	18.5	Dry land	Footslope	
S3-5	29°53'55"	105°47'03"	240	0	1130.3	18.5	Paddy field to dry land	Toeslope	
S4-1	29°46'09"	105°40'25"	408	2	1126.7	18.0	Grassland	Summit	
S4-2	29°46'10"	105°40'24"	403	15	1126.7	18.0	Dry land	Shoulder	
S4-3	29°46'10"	105°40'22"	392	20	1126.7	18.0	Dry land	Backslope	
S4-4	29°46'10"	105°40'22"	396	0	1126.7	18.0	Dry land	Footslope	
S4-5	29°46'14"	105°40'20"	385	0	1126.7	17.9	Dry land	Toeslope	
S5-1	29°44'13"	105°40'19"	421	6	1127.6	18.0	Grassland	Summit	
S5-2	29°44'16"	105°40'19"	406	15	1127.6	18.0	Dry land	Shoulder	
S5-3	29°44'17"	105°40'18"	394	10	1127.6	18.0	Dry land	Backslope	
S5-4	29°44'17"	105°40'19"	396	0	1127.6	18.0	Paddy field to dry land	Footslope	
S5-5	29°44'18"	105°40'17"	387	0	1127.6	18.0	Paddy field to dry land	Toeslope	

Notes: The average annual rainfall of the sampling points was calculated by the annual precipitation data of 1 km resolution in China (2001–2020) (National Earth System Science Data Center, National Science & Technology Infrastructure of China (<http://www.geodata.cn>)); The average annual temperature was calculated by the monthly mean air temperature raster data of China from 2001 to 2020 (1 km resolution) (He et al., 2021).

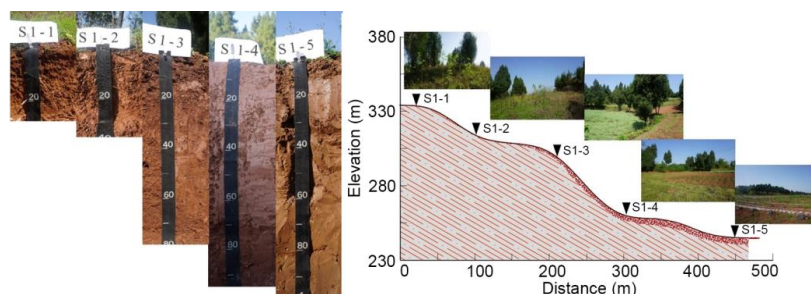


Figure 2. Soil profiles along a toposequence (S1-1, S1-2, S1-3, S1-4, and S1-5 represent the summit, shoulder, backslope, footslope, and toeslope positions of the hillslope, respectively. Take S1 as an example).

2.3 Experimental method and data analysis

The experimental methods used were the same as those used by Tang et al., (2019). In particular, the



127 soil bulk density was determined using the soil core (volume=100 cm³) method and the pipette method
128 was used for soil particle size analysis. A glass electrode was used to measure the soil pH in a 1:2.5
129 soil/water suspension ratio. Soil organic carbon (SOC) content was determined using the
130 dichromate-wet combustion method, and the C/N ratio was calculated as the ratio of SOC to total
131 nitrogen (TN) content (determined by the Kjeldahl method). Cation exchange capacity (CEC) was
132 determined using the Na saturation method. Each sample (0.5 g) was ground at 100 mesh (0.15 mm) in
133 an agate mortar and formulated into a tablet to measure the geochemical elements of the test soil using
134 X-ray fluorescence spectrometry (Sparks et al., 1996; Camobell et al., 2002). These geochemical
135 elements include macroelements, trace elements, rare-earth elements, and radioactive elements. The
136 content and composition characteristics of macroelements are widely used as indicators. Therefore, the
137 geochemical elements in this study refer to the 10 macroelements.

138 Statistical analyses were performed using SPSS 19.0, and included the analysis of paired sample
139 *T*-tests. The distribution map of the sampling sites was drafted using ArcGIS 10.2, and the other
140 diagrams were created using Excel 2016 and Origin 9.3.

141 **3 Results**

142 **3.1 Soil morphology**

143 As shown in Table 2, the profiles with the pattern of A-C horizons were mainly concentrated at the
144 summit and shoulder of the hillslope, the profile at the backslope and footslope was the A-B-C horizon,
145 and the toeslope was the A-B horizon within the excavation depth. From the summit to the toeslope,
146 the soil thickness increased significantly with the change in the soil profile configuration from 16.50 to
147 93.60 cm. In the study area, there were three types of soil colours, including 10R, 2.5YR, and 5YR.
148 The soil texture of horizon C was sandy loam or loam, whereas that of horizon B was mostly clay loam
149 with a few silty loams. The soil texture of horizon A was sandy or silty to clay loam, from the summit
150 to the toeslope (Table 3). The main soil structure of each horizon was blocky or/and granular, and the
151 organic matter accumulation in the surface soil, combined with mechanical ploughing, loosened the
152 soil. A granular structure appeared in the soil, and the structure improved. The cohesiveness of the soil
153 in horizon A was non-sticky, slightly sticky, and sticky from the summit to the toeslope. The



cohesiveness of horizon B was mostly sticky, whereas that of horizon C was mostly non-sticky. Owing to human cultivation or mechanical tillage, there was a small amount of intrusive body in the soil, mainly brick, tile debris, and a small amount of coal cinder. The parent rock of mudstone soil is sedimentary rock, most of which is lacustrine facies sedimentary rock deposited in the Jurassic and Cretaceous periods, therefore, a small number of shells were present in the soil.

Table 2. Morphological attributes of the soil profiles.

Profile No.	Horizon	Depth (cm)	Soil colour		Soil structure	Plasticity	Animal activity	Intrusions
			Dry state	Wet state				
S1-1	Ah	0–12	2.5YR 5/6	2.5YR 4/6	BS	Not plastic	Earthworm	-
	C	>12	2.5YR 5/6	2.5YR 4/6	BS	Not plastic	-	-
S1-2	Ap	0–25	2.5YR 5/4	2.5YR 4/4	GS	Not plastic	-	-
	C	>25	2.5YR 5/6	2.5YR 4/6	BS	Not plastic	-	-
S1-3	Ap	0–18	2.5YR 6/4	2.5YR 4/4	GS, BS	Not plastic	Ant nest	-
	Bw1	18–31/47	2.5YR 5/4	2.5YR 4/4	BS	Slightly plastic	-	Bricks and rubbles
	Bw2	31/47–72	2.5YR 5/4	2.5YR 4/4	BS	Slightly plastic	-	-
	C	>72	2.5YR 5/6	2.5YR 4/6	BS	Not plastic	-	-
S1-4	Ap	0–12	2.5YR 5/3	2.5YR 4/3	BS	Slightly plastic	-	Cinders
	Bw1	12–45	2.5YR 5/3	2.5YR 4/3	BS	Medium plastic	-	Shells
	Bw2	45–70	2.5YR 5/3	2.5YR 4/3	BS	Medium plastic	-	-
	Bw3	70–90	2.5YR 5/3	2.5YR 4/3	BS	Medium plastic	-	-
	C	>90	2.5YR 5/6	2.5YR 4/6	BS	Not plastic	-	-
S1-5	Ap	0–14	2.5YR 6/8	2.5YR 6/8	BS	Slightly plastic	-	Bricks and rubbles
	Bw1	14–30	2.5YR 6/8	2.5YR 5/8	BS	Medium plastic	-	Shells
	Bw2	30–58	2.5YR 6/8	2.5YR 5/8	BS	Medium plastic	-	-
	Bw3	65–100	2.5YR 6/8	2.5YR 5/8	BS	Plastic	-	-
S2-1	Ah	0–10	2.5YR 5/6	2.5YR 4/6	BS	Not plastic	-	-
	C	>10	2.5YR 5/6	2.5YR 4/6	BS	Not plastic	-	-
S2-2	Ap	0–15	2.5YR 5/4	2.5YR 5/6	BS, GS	Not plastic	Earthworm, Centipede	-
	Bw	15–40	2.5YR 5/4	2.5YR 4/4	BS	Not plastic	-	-



Profile No.	Horizon	Depth (cm)	Soil colour		Soil structure	Plasticity	Animal activity	Intrusions
			Dry state	Wet state				
S2-3	C	>40	2.5YR 5/6	2.5YR 4/6	BS	Not plastic	-	-
	Ap	0–24	2.5YR 6/6	2.5YR 6/6	GS	Not plastic	Ant	-
	Bw1	24–35	2.5YR 6/6	2.5YR 5/6	BS, GS	Not plastic	Beetle	-
	Bw2	35–51	2.5YR 6/6	2.5YR 5/6	BS	Slightly plastic	-	-
S2-4	C	>51	2.5YR 5/6	2.5YR 4/6	BS	Not plastic	-	-
	Ap	0–15	2.5YR 5/3	2.5YR 4/3	BS	Not plastic	-	Cinders
	Bw1	15–35	2.5YR 5/3	2.5YR 4/3	BS	Slightly plastic	-	Shells
	Bw2	35–62	2.5YR 5/3	2.5YR 4/3	BS	Medium plastic	-	-
S2-5	Bw3	62–95	2.5YR 5/3	2.5YR 4/3	BS	Medium plastic	-	-
	C	>95	2.5YR 5/6	2.5YR 4/6	BS	Not plastic	-	-
	Ap	0–25	5YR 5/6	5YR 4/6	BS, GS	Slightly plastic	-	-
	Bw1	25–42	5YR 5/4	5YR 4/4	BS	Slightly plastic	-	Shells
S3-1	Bw2	42–70/74	5YR 5/4	5YR 4/4	BS	Medium plastic	-	-
	Bw3	70/74–100	5YR 5/4	5YR 5/4	BS	Medium plastic	-	-
	Ah	0–20/25	2.5YR 5/4	2.5YR 4/4	BS	Not plastic	-	-
	C	>20/25	2.5YR 5/6	2.5YR 4/6	BS	Not plastic	-	-
S3-2	Ap	0–20	2.5YR 5/4	2.5YR 6/6	GS	Not plastic	Earthworm	-
	Bw1	20–33	2.5YR 5/4	2.5YR 6/6	GS	Not plastic	-	-
	Bw2	33–60	2.5YR 5/4	2.5YR 6/6	BS	Slightly plastic	-	-
	C	>60	2.5YR 5/6	2.5YR 4/6	GS	Not plastic	-	-
S3-3	Ap	0–22	2.5YR 6/4	2.5YR 4/4	GS	Not plastic	-	-
	Bw1	22–37	2.5YR 5/4	2.5YR 4/4	BS, GS	Not plastic	-	Bricks
	Bw2	37–75	2.5YR 5/4	2.5YR 4/4	BS	Slightly plastic	-	-
	C	>75	2.5YR 5/6	2.5YR 4/6	BS	Not plastic	-	-
S3-4	Ap	0–15	2.5YR 5/3	2.5YR 4/3	BS	Slightly plastic	Ant	-
	Bw1	15–38	2.5YR 5/3	2.5YR 4/3	BS	Slightly plastic	-	-
	Bw2	38–75	2.5YR 5/3	2.5YR 4/3	BS	medium	-	-
	Bw3	75–100	2.5YR 5/3	2.5YR 4/3	BS	Medium	-	-



Profile No.	Horizon	Depth (cm)	Soil colour		Soil structure	Plasticity	Animal activity	Intrusions
			Dry state	Wet state				
S3-5	Ap	0–18	5YR 5/6	5YR 4/6	BS	plastic Slightly plastic	Earthworm	-
	Bw1	18–33	5YR 5/4	5YR 4/4	BS	Medium plastic	-	-
	Bw2	33–56	5YR 5/4	5YR 4/4	BS	Plastic	-	-
	Bw3	56–84	5YR 5/4	5YR 5/4	BS	Plastic	-	-
	Bw4	84–100	5YR 4/4	5YR 3/4	BS	Plastic	-	-
S4-1	Ah	0–20	10R 5/4	10R 4/4	BS	Not plastic	-	-
	C	>20	10R 4/4	10R 3/4	BS	Not plastic	-	-
S4-2	Ap	0–25	10R 5/4	10R 4/4	GS	Not plastic	Earthworm	-
	Bw	25–40	10R 4/4	10R 3/4	GS	Slightly plastic	-	-
	C	>40	10R 4/4	10R 3/4	BS	Not plastic	-	-
S4-3	Ap	0–20	2.5YR 5/6	2.5YR 4/6	BS	Not plastic	-	-
	Bw	20–40/55	2.5YR 5/6	2.5YR 4/6	BS	Medium plastic	-	-
	C	>40/55	2.5YR 4/6	2.5YR 3/6	BS	Not plastic	-	-
S4-4	Ap	0–20	2.5YR 5/3	2.5YR 4/3	GS, BS	Not plastic	Ant	-
	AB	20–35	2.5YR 4/3	2.5YR 4/3	BS	Not plastic	-	-
	Bw1	35–51	2.5YR 4/3	2.5YR 4/3	BS	Medium plastic	-	Cinders
	Bw2	51–83	2.5YR 4/3	2.5YR 4/3	BS	Medium plastic	-	-
S4-5	C	>83	2.5YR 4/4	2.5YR 3/4	BS	Not plastic	-	-
	Ap	0–20	2.5YR 5/3	2.5YR 4/3	BS, GS	Not plastic	Earthworm	-
	Bw1	20–45	2.5YR 5/3	2.5YR 4/3	BS	Medium plastic	-	Shells
	Bw2	45–68/75	2.5YR 5/3	2.5YR 4/3	BS	Medium plastic	-	-
	Bw3	68/75–100	2.5YR 4/3	2.5YR 4/3	BS	Medium plastic	-	-
S5-1	Ah	0–18	10R 5/6	10R 4/6	GS	Not plastic	-	-
	C	>18	10R 4/6	10R 3/6	BS	Not plastic	-	-
S5-2	Ap	0–10/15	10R 5/6	10R 4/6	GS	Not plastic	Earthworm, Centipede	-
	AC	10/15–25	10R 5/6	10R 4/6	BS	Not plastic	-	-
	C	>25	10R 4/6	10R 3/6	BS	Not plastic	-	-
S5-3	Ap	0–22	2.5YR 5/6	2.5YR 4/6	BS	Not plastic	-	-
	AB	22–45	2.5YR 5/6	2.5YR 4/6	BS	Slightly	-	-



Profile No.	Horizon	Depth (cm)	Soil colour		Soil structure	Plasticity	Animal activity	Intrusions
			Dry state	Wet state				
S5-4	Bw	45–65	2.5YR 5/6	2.5YR 4/6	BS	plastic Medium	-	Cinders
	C	>65	2.5YR 4/6	2.5YR 3/6	BS	plastic Not plastic	-	-
	Ap	0–10	2.5YR 5/3	2.5YR 4/3	BS	Slightly plastic	Ant nest	Cinders
	Bw1	10–30	5YR 6/4	5YR 4/6	BS	Medium plastic	-	Shells
	Bw2	30–55	2.5YR 4/3	2.5YR 4/3	BS	Medium plastic	-	-
S5-5	Bw3	55–68	2.5YR 4/3	2.5YR 4/3	BS	Plastic	-	-
	Bw4	68–100	2.5YR 4/4	2.5YR 3/4	BS	Plastic	-	-
	Ap	0–30	5YR 5/6	5YR 4/6	BS	Not plastic	Earthworm	-
	Bw1	30–55	5YR 5/4	5YR 4/4	BS	Medium plastic	-	Shells
	Bw2	55–77	5YR 5/4	5YR 4/4	BS	Medium plastic	-	-
	Bw3	77–100	5YR 5/4	5YR 5/4	BS	Plastic	-	-

160 Notes: BS, blocky structure; GS, granular structure.



As shown in Fig. 3, there were significant differences in the redness rating (RR) index between different slope positions and horizons. According to the analysis of the RR index, slope position had a significant effect on soil development. The RR index was relatively low in the whole region. The maximum value of the RR index appeared in the parent material (C horizon), which indicated that aluminium enrichment was weak in the process of soil development in this region, and the soil development was relatively young. The RR index decreased from summit to toeslope, and that of the footslope and toeslope were similar, with average values of 7.10 and 7.97, respectively. From the profile horizon, the average RR index of the soil profile at different slope positions was in the following order: horizon C > A > B (Fig. 3). The soil profile in horizon A was mainly affected by farming, and that in horizon B was affected by topography. The soil redness rating varied greatly among soil horizons, and the degree of soil development also differed.

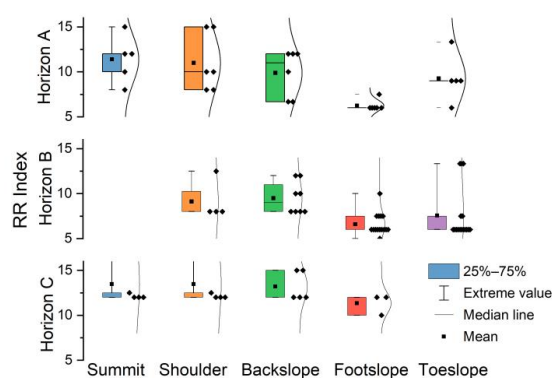


Figure 3. RR index of soil profiles in different slope positions.

3.2 Soil physical and chemical properties

The bulk density and porosity of the soil profiles at different slope positions were shown in Table 3. The bulk density in horizons A and B of the soil profiles increased gradually from the summit to the toeslope. The bulk density of the soil profiles at different slope positions showed that horizon A was smaller than horizon B. The reason for this is that, during the process of soil development, the aggregates of horizon A are in good condition with the accumulation of organic matter and an increase in clay content. However, the soil in horizon B is compacted owing to disturbance during human cultivation, and the bulk density then increases. The porosity in horizons A and B of the soil profiles



decreased gradually from the summit to the toeslope. The porosity of horizon A was higher than that of horizon B. As shown in Table 3, the share of sand and silt fractions in horizons A and B decreased gradually from the summit to the toeslope. The clay fraction content in horizons A and B increased gradually from the summit to the toeslope.

Table 3. The bulk density, porosity, and particle size distribution of soil profiles at different slope positions.

Slope position	Horizon	Bulk density (g cm ⁻³)	Porosity (%)	Particle size distribution (%)		
				Clay	Silt	Sand
Summit	A	1.35±0.09	46.36±3.44	14.26±2.23	47.14±8.51	38.60±9.37
	C	/	/	10.99±3.73	40.21±1.88	48.80±2.95
Shoulder	A	1.37±0.11	45.5±4.82	17.25±2.72	44.65±3.33	38.09±4.95
	B	1.38±0.03	46.97±1.47	19.59±3.60	40.52±3.95	39.90±2.00
	C	/	/	10.39±1.88	39.26±1.53	50.35±3.14
Backslope	A	1.36±0.12	45.41±5.56	21.81±2.99	41.13±3.31	37.07±5.52
	B	1.48±0.14	42.41±5.20	22.14±4.08	39.90±5.30	37.96±5.89
	C	/	/	10.54±1.63	38.96±0.94	50.49±1.93
Footslope	A	1.43±0.04	43.32±1.80	30.82±4.19	39.33±1.96	29.85±4.01
	B	1.52±0.09	41.33±3.72	29.13±3.64	39.87±3.54	31.00±5.22
	C	/	/	10.13±1.52	39.60±0.98	50.27±2.11
Toeslope	A	1.53±0.16	39.64±6.09	36.47±3.47	38.79±1.96	24.74±4.20
	B	1.60±0.09	37.72±3.80	36.54±1.28	38.91±3.15	24.55±3.87

As shown in Fig. 4, the pH of horizon A and B was significantly higher at the summit, shoulder, and backslope than that at the footslope and toeslope; however, there was no significant difference in the pH of horizon C at different slope positions. The SOC content in horizon C was low, and there was no significant difference among the different slope positions. The SOC content in horizons A and B gradually increased with decreasing slope elevation and the difference in SOC above and below the backslope was significant. The accumulation of SOC in horizon A at the footslope and toeslope was mainly due to artificial cultivation and fertilisation, while the accumulation of SOC in horizon B was mainly caused by detachment, transportation, accumulation, and burial of deep soil in the higher topography. The hilly terrain was conducive to the accumulation of SOC content at the footslope and toeslope. Part of the P in the soil comes from the parent rock, whereas the other part comes from the application of chemical fertilisers and plant decomposition. As a highly mobile element, P easily migrates in the lower horizon of the soil surface, whereas it is enriched in the surface horizon of soil (Fig. 4). Total phosphorus (TP) in the soil at the summit of the slope was significantly lower than that



in the footslope and toeslope. The TP in the soil above the backslope was in the order of horizon B > C > A, whereas that in the footslope and toeslope was A > B > C. The TN content from the summit to the toeslope increased with decreasing slope elevation, and there was a significant difference above and below the backslope, indicating that there was TN accumulation at the foot and toeslope. In general, the TN above the backslope was in the order of horizon A > B > C of the soil profile, whereas that of the footslope and toeslope was horizon B > A > C (Fig. 4). The total potassium (TK) content from the summit to the toeslope gradually increased with increasing slope elevation. There was a significant difference between the summit, shoulder of the slope and footslope, and toeslope, indicating that K in the soil accumulated at a lower topographic position. According to the different horizons, the TK in the soil above the backslope was in the order of horizon C > A > B, whereas that at the footslope was horizon A > C > B (Fig. 4). There were differences in the CEC content among the different soil horizons. The average CEC contents in horizons A, B, and C were 27.37, 29.67, and 28.36 cmol(+) kg⁻¹, respectively. These results indicate that cations migrated and leached in horizon A and accumulated and were enriched in horizon B. The CEC above the backslope was in the order of horizon C > B > A, whereas that below the backslope was B > A > C.

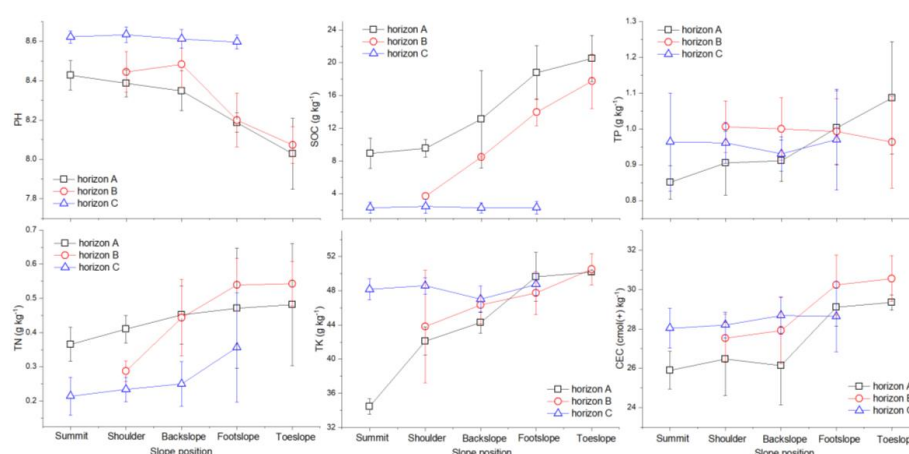


Figure 4. Chemical properties of soil profiles at different slope positions.

3.3 Geochemical composition and chemical weathering indices

In general, the footslope and toeslope of the hillslope showed accumulation of Al, Fe, Mg, and K, and leaching loss of Ca, Na, and Si compared with the summit and shoulder of the hillslope. There was



a leaching loss of K in horizon A at the summit of the hillslope, while the variation in elements in each horizon at the shoulder of the hillslope was not obvious (Fig. 5).

The leaching of Si and Na was obvious in horizon B of the slope profile, and the accumulation of Al, Fe, and Mg was significant in horizon B of the slope profile relative to horizon C. The leaching of Na and Ca was significant in horizons A and B, whereas the leaching of Ca and Na was obvious in horizon B relative to horizon A in the hillslope. During the development of silicate soils, Na and Ca were leached first, followed by K, Si was leached in the late stage, and Al and Fe were relatively enriched. The soil in this study was in the stage of leaching of Ca and Na, the leaching of soil geochemical elements was not strong, and the degree of soil development was weak. The effect of microtopography on soil chemical weathering was greater than that on the profile.

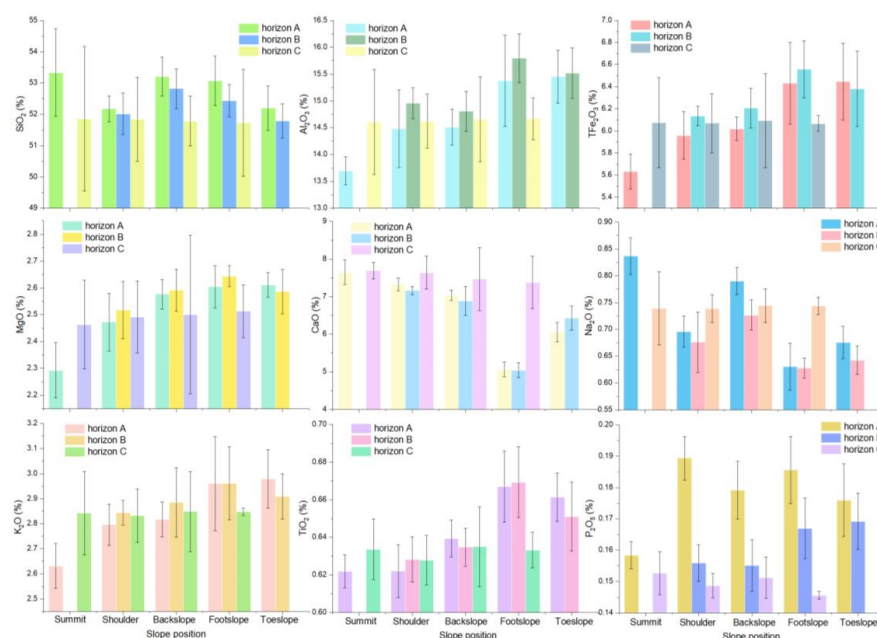
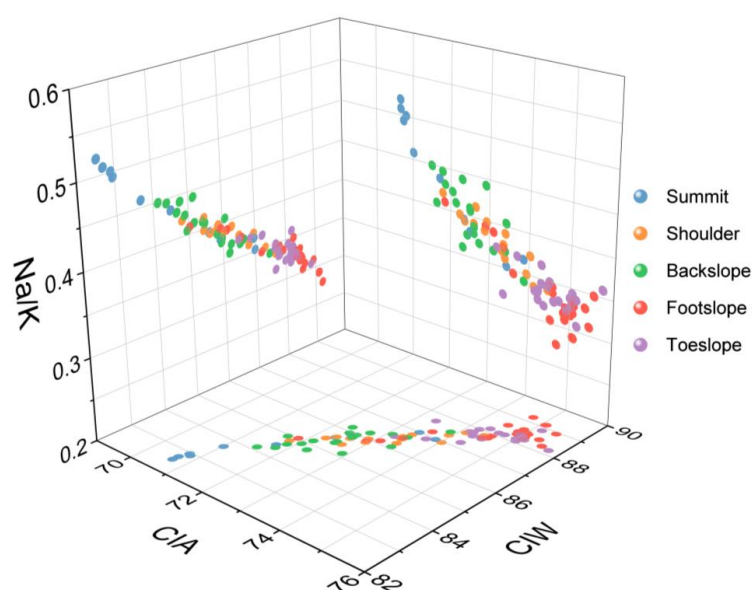


Figure 5. Geochemical element contents of soil profiles at different positions.

The chemical index of alteration (CIA) values were 71.78, 73.17, 72.51, 74.55, and 74.55 from summit to toeslope. Moreover, there were significant differences in CIA values between horizons A and B at the summit, shoulder, backslope, footslope, and toeslope. The CIA values of horizons A, B, and C were 72.92, 74.37, and 72.61, respectively. The variation trend of chemical index of weathering (CIW) was basically the same as that of CIA, while the indication effects of CIA and CIW to reflect the degree of soil weathering were the same. Correlation analysis of CIA, CIW, and Na/K showed that



239 there was a significant negative correlation between Na/K and CIA and CIW (Fig. 6). The CIA, CIW,
240 and Na/K values indicated that the soil in the study area had moderate chemical weathering, and the
241 chemical weathering of the soil parent horizon remained at the same level from the summit to the
242 toeslope of the hillslope. Horizons A and B showed a trend of first increasing and then decreasing with
243 decreasing slope elevation, and the soil of horizon B at the footslope had the highest degree of
244 development, which indicated that the soil was strongly detached and transported under the action of
245 microtopography, and the deeply weathered soil in higher terrain was deposited into the soil of horizon
246 B at the footslope.

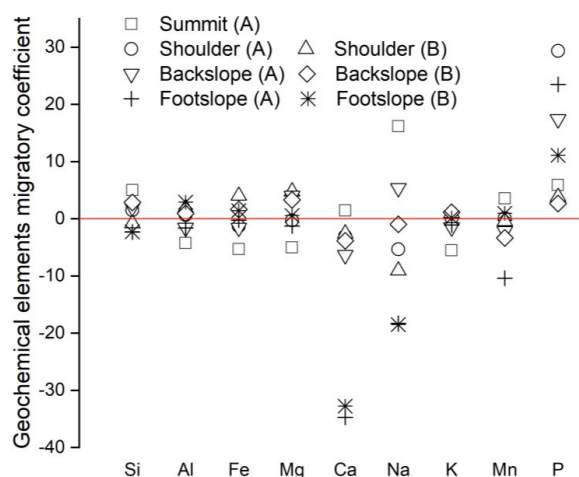


247
248 **Figure 6.** Chemical weathering parameters of soil profiles at different positions.

249 As shown in Fig. 7, the mobility of the elements varies at different microtopographical positions.
250 The migration directions of Ca and Na at the summit and backslope were completely opposite to that at
251 the footslope. The average migration coefficients of Ca at the summit, backslope, and footslope were
252 1.43%, -4.93%, and -33.43%, respectively, while the average migration coefficients of Na were
253 16.15%, 1.73%, and -18.43%, respectively, and the migration direction changed from enrichment to
254 leaching. Al, Fe, and Mg were first leached and then enriched from the summit to the footslope, which
255 may be due to the higher sand content in the soil and relatively large intergranular pores, resulting in
256 the loss of elements under the action of rainfall and underground runoff. However, where the terrain
257 was relatively low, such as the footslope, the water condition was sufficient, which provided conditions



for soil chemical weathering, and Ca and Na leached out, while Al and Fe were enriched.



259

260 **Figure 7.** Geochemical elements migratory coefficient of soil profiles at different slope positions.

261 3.4 Mineralogy characteristics

262 The mineral composition of the soils was analysed using X-ray diffraction (Fig. 8). There was an
 263 evident mineralogical similarity between the soils at different slope positions and horizons. The
 264 mudstone soils in this study were dominated by illite, kaolinite, and an illite/smectite mixed horizon,
 265 and the mineral composition of the soils was the same as that of their parent rock. These results
 266 indicate that the clay minerals in the soils originated mostly from the parent material and that they were
 267 only slightly influenced by soil-forming processes.

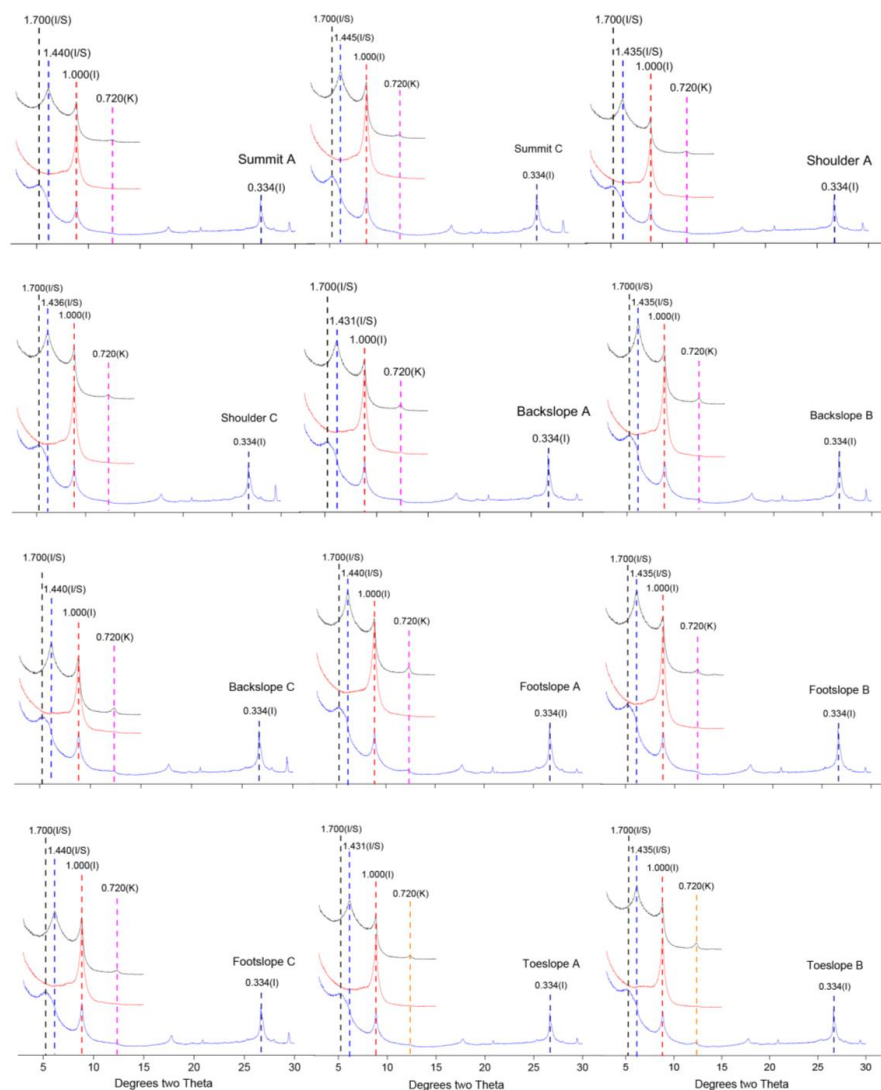


Figure 8. X-ray diffraction data for soils at different slope positions (A–horizon A, B–horizon B, and C–horizon C). The sequence of treatments is represented by three different colours: the black (top), red (middle position), and blue (bottom) curves represent the air-dried mount (AD) samples, samples heated at 550 °C (K550), and glycol solvated (EG) samples, respectively. I: illite; K: kaolinite; I/S: illite/smectite mixed-horizon.

4 Discussion



4.1 Microtopography affects the chemical weathering of the soil at different slope positions

As shown in Table 4, there was a significant negative correlation between sand content and SOC, TN, TK, CEC, and bulk density and a significant positive correlation between sand content and pH and porosity. There was a significant negative correlation between silt content and SOC, TN, TP, TK, and CEC, and a significant positive correlation between silt content and pH. There was a negative correlation between clay content and pH and porosity, and a significant positive correlation between clay content and SOC, TN, TK, CEC, and bulk density. There is a significant correlation between the particle composition and amorphous Fe and Al content (Obi, 2015), particularly the clay content. Amorphous Fe can provide a high specific surface area to influence ion adsorption in soil, whereas Al participates in hydrolysis to that influence soil pH (Harter, 2007). The lower alkali metals in the soil increased the H^+ on the mineral surface, resulting in the destruction of the mineral structure and the release of other mineral ions, such as Si^{4+} , Fe^{3+} , and Al^{3+} . The released Fe^{3+} and Al^{3+} formed hydrated oxides under appropriate conditions and remained in the soil solution. Finally, the amorphous hydrated oxides of aluminium and iron, together with kaolinite, become the main solids in the soil. That is, feldspar is rearranged by Si and Al under weathering to form clay minerals such as kaolinite, which explains the relationship between particle composition and hydrated oxides. Therefore, the particle composition, particularly the clay content, is an important variable that affects the decisive factors of soil characteristics.

Table 4. Pearson's correlation coefficients of soil physical and chemical properties.

	SP	pH	SOC	TN	TP	TK	CEC	BD	Porosity	Sand	Silt	Clay
SP	1											
pH	-0.328**	1										
SOC	0.170	-0.605**	1									
TN	0.172	-0.530**	0.688**	1								
TP	0.079	-0.221	0.156	0.191	1							
TK	0.419**	-0.609**	0.500**	0.496**	0.373**	1						
CEC	0.469**	-0.422**	0.532**	0.433**	0.173	0.564**	1					
BD	0.400**	-0.354**	0.382**	0.363**	0.088	0.522**	0.436**	1				
Porosity	-0.323**	0.357**	-0.422**	-0.370**	-0.054	-0.478**	-0.354**	-0.977*	1			
Sand	-0.255*	0.531**	-0.618**	-0.428**	-0.086	-0.515**	-0.500**	-0.557**	0.565**	1		
Silt	-0.265*	0.340**	-0.277*	-0.300*	-0.275*	-0.457**	-0.356**	-0.100	0.054	-0.161	1	
Clay	0.383**	-0.680**	0.725**	0.562**	0.232	0.730**	0.661**	0.573**	-0.555**	-0.839**	-0.402**	1

Notes: SP, slope position; BD, bulk density; *, $p \leq 0.05$; **, $p \leq 0.01$.

The degree of soil chemical weathering varied with changes in the slope position and soil depth.



296 According to the variance F value of the soil chemical weathering index under different factors (Table
297 5), the CIA, CIW, and Na/K of soils varied significantly between different horizons at different slope
298 positions and the interaction between slope position and horizon. Therefore, topographic changes
299 caused differences in chemical weathering of the soil profile, mainly because the soil at the top and
300 shoulder of the slope was mostly developed under natural conditions, and soil weathering mainly
301 depended on the change in natural hydrothermal status and the effect of soil organisms. The return of
302 nutrient elements such as Na, Ca, and Mg by litter may decelerate the chemical weathering process,
303 thus decelerating soil development in the middle and upper hills. At the footslope and other relatively
304 low topographic locations, soil moisture is retained, which provides moisture conditions for chemical
305 weathering. The depth of the soil profile at the footslope was more than 1 m, and a small or moderate
306 number of rust spots began to appear in the soil horizon, resulting in changes in the soil profile
307 morphology and chemical characteristics. Meanwhile, the soil on the footslope and toeslope was
308 affected by human cultivation. Irrigation changes the soil moisture status, tillage changes soil aeration
309 conditions (Wei et al., 2006), and fertilisation increases soil nutrient elements. These factors promote
310 soil mineral weathering and element leaching, and soil erosion intensifies (He et al., 2007; Ni and
311 Zhang, 2007; Zheng et al., 2007). Therefore, soil erosion caused by tillage promotes chemical
312 weathering in the soil. In areas with large terrain slopes, the degree of physical rock erosion is greater,
313 and chemical weathering is stronger (Gabet, 2007; Riebe et al., 2004).

314 **Table 5.** Analysis of variance F value of chemical weathering indicators of soils at different slope
315 positions and horizons.

Factor	CIA		CIW		Na/K	
	F	Sig.	F	Sig.	F	Sig.
Slope position	27.298	0.000	29.754	0.000	23.191	0.000
Occurrence layer	19.951	0.000	16.077	0.000	8.985	0.000
$S \times O$	7.222	0.000	9.223	0.000	8.506	0.000

316 Notes: $S \times O$, interaction of slope position and horizon.

317 **4.2 The redistribution of water and materials by microtopography resulted in the difference of** 318 **pedogenic characteristics at different slope positions**

319 Water flow runs through the entire process of soil occurrence and development. Water plays an
320 important role in soil formation as the main medium for transporting solids and ions in the soil
321 (Schaetzl and Anderson, 2005). Microtopography dominates surface hydrological processes and affects



322 water redistribution (Muscarella et al., 2020; Peñuela et al., 2015; Wang et al., 2022), resulting in
323 differences in the physicochemical properties of soil at different slope positions (Maranhão et al., 2020).
324 Therefore, even in a microdomain of tens of meters, the soil of the same genus also forms different
325 textures owing to the difference in properties. In this study, the physicochemical properties of the soil
326 varied with the change in the slope position, particularly between the soil above and below the
327 backslope, and there were also differences among the different horizons. From the summit to toeslope,
328 the sand content of the soil gradually decreased, and the clay content of the soil gradually increased.
329 The mudstone parent rock exposed at the summit of the hilly mountainous region caused by erosion is
330 rich clay minerals and has strong water absorption capacity, therefore, it is easily physically weathered
331 under the influence of moist heat expansion. Consequently, stony subsoil is frequently formed at or
332 near the summit of the slope (Zhong et al., 2020). Obi et al., (2014) showed that sand content is
333 affected by rainfall and infiltration. When rainfall exceeded infiltration, it caused redistribution of sand
334 in the slope and soil horizon. This phenomenon is often observed in thunderstorm weather, which
335 reduces the stability of soil on the slope surface (Eneje et al., 2007; Oguike and Mbagwu, 2009). The
336 results of this study also showed that the degree of chemical weathering of horizon A at the footslope
337 and toeslope was lower than that of horizon B, which was mainly due to the redistribution of soil
338 materials by microtopography (Baltensweiler et al., 2020). Soil and water loss is serious in hilly
339 mountainous regions, and the materials transported by upper erosion are deposited at the footslope and
340 toeslope. Long-term contact between water and sediment leads to further chemical action, resulting in
341 soil with high organic matter content and fine texture, which is buried by a new round of denudation
342 accumulation and self-weathered soil, becoming a B-horizon soil with a higher degree of development
343 than the topsoil.

344 **5 Conclusion**

345 Five soil profiles along the slopes were sampled at the summit, shoulder, backslope, footslope, and
346 toeslope positions on behalf of the microtopography. The morphological characteristics,
347 physiochemistry, and geochemical attributes of the profiles were analysed. The results indicate that the
348 morphological characteristics of the mudstone soil profile were mainly inherited and affected by the
349 parent material. There was a significant correlation between the soil and parent material developed at



350 different slope positions. Under the effect of topography, different parts of the hillslope exhibited
351 different profile morphologies. From the summit to the toeslope, the profile configuration of the
352 mudstone soil changed from A-C to A-B-C, and the thickness of the soil increased. The bulk density,
353 clay fraction, soil organic matter, TN, TP, TK, and CEC increased from the summit to the toeslope of
354 the hillslope, whereas the pH, porosity, sand, and silt fraction decreased. From the perspective of soil
355 element migration, the migration of geochemical elements differed at different topographic locations.
356 The migration direction of Ca and Na at the summit, backslope, and footslope changed from
357 enrichment to leaching, whereas that of Al, Fe, and Mg changed from leaching to enrichment. In
358 addition to the parent material, the development of mudstone soil is significantly related to
359 microtopographic action. At the summit and shoulder of the hillslope, weathered materials are
360 transported away by gravity and surface erosion, and new rocks are often exposed; therefore the
361 characteristics of soil development is relatively weak. Alternatively, in flat areas such as the footslope
362 and toeslope with sufficient water conditions, the long-term contact between water, soil, and sediment
363 leads to further chemical weathering, resulting in a higher degree of soil development.
364 Microtopography can affect physicochemical properties, chemical weathering, and redistribution of
365 water and materials, resulting in differences in pedogenic characteristics at different slope positions.

366 **Data availability**

367 All raw data can be obtained from the corresponding authors on request.

368 **Author contributions**

369 Conceptualization, Banglin Luo and Jiangwen Li; investigation and data curation, Banglin Luo,
370 Jiangwen Li and Jiahong Tang; methodology and formal analysis, Banglin Luo, Jiangwen Li and
371 Jiahong Tang; writing-original draft preparation, Banglin Luo; writing-review and editing, Jiangwen Li,
372 Chaofu Wei and Shouqin Zhong; project administration and supervision, Chaofu Wei and Shouqin
373 Zhong; funding acquisition, Chaofu Wei and Shouqin Zhong.

374 **Competing interests**

375 The authors declare that they have no conflict of interest.



376 **Acknowledgements**

377 This study was supported by the Fundamental Research Funds for the National Natural Science
378 Foundation of China (42077007), and the Startup Project of Doctor Scientific Research at Southwest
379 University (No. SWU120065). Acknowledgement for the data support from "National Earth System
380 Science Data Center, National Science & Technology Infrastructure of China.
381 (<http://www.geodata.cn>)".

382 **References**

- 383 Baltensweiler, A., Heuvelink, G. B. M., Hanewinkel, M., and Walthert, L.: Microtopography shapes
384 soil pH in flysch regions across Switzerland, *Geoderma*, 380, 114663,
385 <https://doi.org/10.1016/j.geoderma.2020.114663>, 2020.
- 386 Botschek, J., Ferraz, J., Jahnel, M., and Skowronek, A.: Soil chemical properties of a toposequence
387 under primary rain forest in the Itacoatiara vicinity (Amazonas, Brazil), *Geoderma*, 72, 119–132,
388 [https://doi.org/10.1016/0016-7061\(96\)00026-2](https://doi.org/10.1016/0016-7061(96)00026-2), 1996.
- 389 Brubaker, S. C., Jones, A. J., Lewis, D. T., and Frank, K.: Soil Properties Associated with Landscape
390 Position, *Soil Science Society of America Journal*, 57, 235–239,
391 <https://doi.org/10.2136/sssaj1993.03615995005700010041x>, 1993.
- 392 Camobell, G. S., Horton, R., Jury, W. A., Nielsen, D. R., van Es, H. M., Wierenga, P. J., Dane, J. H.
393 and Topp, G. C.: *Methods of Soil Analysis, Part 4: Physical Methods*, Number 5 in the Soil Science
394 Society of America Book Series, Soil Science Society of America, Madison, Wisconsin, USA, 2002.
- 395 Darmody, R. G., Thorn, C. E., and Allen, C. E.: Chemical weathering and boulder mantles,
396 *Kärkevagge, Swedish Lapland, Geomorphology*, 67, 159–170,
397 <https://doi.org/10.1016/j.geomorph.2004.07.011>, 2005.
- 398 Eneje, R.C. and Adanma, N.: Percent Clay, Aggregate Size Distribution and Stability with Depth
399 Along Atoposequence Formed on Coastal Plain Sands, *Online Journal of Earth Sciences*, 1, 108–112,
400 2007.
- 401 Gabet, E. J.: A theoretical model coupling chemical weathering and physical erosion in
402 landslide-dominated landscapes, *Earth and Planetary Science Letters*, 264, 259–265,
403 <https://doi.org/10.1016/j.epsl.2007.09.028>, 2007.



- 404 Harter, R.D.: Acid Soils of the Tropics, North Fort Myers: ECHO Community, 2007.
- 405 He, C., Wang, M., Liu, K., Li, K., and Jiang, Z.: GPRChinaTemp1km: 1 km monthly mean air
406 temperature for China from January 1951 to December 2020 [Data set], In Earth System Science
407 Data, 14(7), 3273–3292, Zenodo, <https://doi.org/10.5281/zenodo.5111989>, 2021.
- 408 He, X., Xu, Y., and Zhang, X.: Traditional farming system for soil conservation on slope farmland in
409 southwestern China, Soil and Tillage Research, 94, 193–200,
410 <https://doi.org/10.1016/j.still.2006.07.017>, 2007.
- 411 IUSS Working Group WRB.: World Reference Base for Soil Resources, International soil
412 classification system for naming soils and creating legends for soil maps, 4th edition, International
413 Union of Soil Sciences (IUSS), Vienna, Austria, 2022.
- 414 Kokulan, V., Akinremi, O., Moulin, A. P., and Kumaragamage, D.: Importance of terrain attributes in
415 relation to the spatial distribution of soil properties at the micro scale: a case study, Can. J. Soil. Sci.,
416 98, 292–305, <https://doi.org/10.1139/cjss-2017-0128>, 2018.
- 417 Leguédais, S., Séré, G., Auclerc, A., Cortet, J., Huot, H., Ouvrard, S., Watteau, F., Schwartz, C., and
418 Morel, J. L.: Modelling pedogenesis of Technosols, Geoderma, 262, 199–212,
419 <https://doi.org/10.1016/j.geoderma.2015.08.008>, 2016.
- 420 Luo, J., Zheng, Z., Li, T., and He, S.: Spatial variation of microtopography and its effect on temporal
421 evolution of soil erosion during different erosive stages, CATENA, 190, 104515,
422 <https://doi.org/10.1016/j.catena.2020.104515>, 2020.
- 423 Lv, W., Liu, Y., Du, J., Tang, L., Zhang, B., Liu, Q., Cui, X., Xue, K., and Wang, Y.: Microtopography
424 mediates the community assembly of soil prokaryotes on the local-site scale, CATENA, 222, 106815,
425 <https://doi.org/10.1016/j.catena.2022.106815>, 2023.
- 426 Maranhão, D. D. C., Pereira, M. G., Collier, L. S., Anjos, L. H. C. dos, Azevedo, A. C., and Cavassani,
427 R. de S.: Pedogenesis in a karst environment in the Cerrado biome, northern Brazil, Geoderma, 365,
428 114169, <https://doi.org/10.1016/j.geoderma.2019.114169>, 2020.
- 429 Muscarella, R., Kolyaie, S., Morton, D. C., Zimmerman, J. K., and Uriarte, M.: Effects of topography
430 on tropical forest structure depend on climate context, Journal of Ecology, 108, 145–159,
431 <https://doi.org/10.1111/1365-2745.13261>, 2020.
- 432 Nagamatsu, D., Hirabuki, Y., and Mochida, Y.: Influence of micro-landforms on forest structure, tree
433 death and recruitment in a Japanese temperate mixed forest: Influence of landforms on a Japanese



- 434 forest, *Ecological Research*, 18, 533–547, <https://doi.org/10.1046/j.1440-1703.2003.00576.x>, 2003.
- 435 Nation Soil Survey Center, Natural Resources Conservation Service, and U. S. Department of
- 436 Agriculture.: *Field Book for Describing and Sampling Soils*, Version 3.0, Spi. ed., Government
- 437 Printing Office, Lincoln, Nebraska, USA, 2013.
- 438 Ni, S. J. and Zhang, J. H.: Variation of chemical properties as affected by soil erosion on hillslopes and
- 439 terraces, *Eur J Soil Science*, 58, 1285–1292, <https://doi.org/10.1111/j.1365-2389.2007.00921.x>,
- 440 2007.
- 441 Obi, J. C., Ogban, P. I., Ituen, U. J., and Udoh, B. T.: Development of pedotransfer functions for
- 442 coastal plain soils using terrain attributes, *CATENA*, 123, 252–262,
- 443 <https://doi.org/10.1016/j.catena.2014.08.015>, 2014.
- 444 Obi, J. C.: Particle size fractions and pedogenesis of coastal plain sands, *Archives of Agronomy and*
- 445 *Soil Science*, 61, 1473–1490, <https://doi.org/10.1080/03650340.2015.1006201>, 2015.
- 446 Oguike, P. C. and Mbagwu, J. S. C.: Variations in Some Physical Properties and Organic Matter
- 447 Content of Soils of Coastal Plain Sand under Different Land Use Types, 7, 2009.
- 448 Pal, D. K., Srivastava, P., Durge, S. L., and Bhattacharyya, T.: Role of microtopography in the
- 449 formation of sodic soils in the semi-arid part of the Indo-Gangetic Plains, India, *CATENA*, 51, 3–31,
- 450 [https://doi.org/10.1016/S0341-8162\(02\)00092-9](https://doi.org/10.1016/S0341-8162(02)00092-9), 2003.
- 451 Parent, A. C., Bélanger, M. C., Parent, L. E., Santerre, R., Viau, A. A., Anctil, F., Bolinder, M. A., and
- 452 Tremblay, C.: Soil properties and landscape factors affecting maize yield under wet spring
- 453 conditions in eastern Canada, *Biosystems Engineering*, 99, 134–144,
- 454 <https://doi.org/10.1016/j.biosystemseng.2007.10.006>, 2008.
- 455 Peñuela, A., Javaux, M., and Bièlders, C. L.: How do slope and surface roughness affect plot-scale
- 456 overland flow connectivity?, *Journal of Hydrology*, 528, 192–205,
- 457 <https://doi.org/10.1016/j.jhydrol.2015.06.031>, 2015.
- 458 Phillips, J. D., Turkington, A. V., and Marion, D. A.: Weathering and vegetation effects in early stages
- 459 of soil formation, *CATENA*, 72, 21–28, <https://doi.org/10.1016/j.catena.2007.03.020>, 2008.
- 460 Riebe, C. S., Kirchner, J. W., and Finkel, R. C.: Erosional and climatic effects on long-term chemical
- 461 weathering rates in granitic landscapes spanning diverse climate regimes, *Earth and Planetary*
- 462 *Science Letters*, 224, 547–562, <https://doi.org/10.1016/j.epsl.2004.05.019>, 2004.
- 463 Salako, F. K., Dada, P. O., Adejuyigbe, C. O., Adedire, M. O., Martins, O., Akwuebu, C. A., and



- 464 Williams, O. E.: Soil strength and maize yield after topsoil removal and application of nutrient
465 amendments on a gravelly Alfisol toposequence, *Soil and Tillage Research*, 94, 21–35,
466 <https://doi.org/10.1016/j.still.2006.06.005>, 2007.
- 467 Schaetzl, R., and Anderson, S.: *Soils: Genesis and Geomorphology*, Cambridge University Press, New
468 York, USA, 2005.
- 469 Sparks, D.L., Page, A.L., Helmke P.A., Loeppert, R.H., Soltanpour, P.N., Tabatabai, M.A., Johnston,
470 C.T., and Sumner, M.E.: *Methods of Soil Analysis, Part 3: Chemical Methods*, Number 5 in the Soil
471 Science Society of America Book Series, Soil Science Society of America and American Society of
472 Agronomy, Madison, Wisconsin, USA, 1996.
- 473 Tang, J., Han, Z., Zhong, S., Ci, E., and Wei, C.: Changes in the profile characteristics of cultivated
474 soils obtained from reconstructed farming plots undergoing agricultural intensification in a hilly
475 mountainous region in southwest China with regard to anthropogenic pedogenesis, *CATENA*, 180,
476 132–145, <https://doi.org/10.1016/j.catena.2019.04.020>, 2019.
- 477 Thompson, S. E., Katul, G. G., and Porporato, A.: Role of microtopography in rainfall-runoff
478 partitioning: An analysis using idealized geometry, *Water Resour. Res.*, 46,
479 <https://doi.org/10.1029/2009WR008835>, 2010.
- 480 Veneman, P. L. M., Jacke, P. V., and Bodine, S. M.: Soil formation as affected by pit and mound
481 microrelief in Massachusetts, USA, *Geoderma*, 33, 89–99,
482 [https://doi.org/10.1016/0016-7061\(84\)90022-3](https://doi.org/10.1016/0016-7061(84)90022-3), 1984.
- 483 Vidal Vázquez, E., Vivas Miranda, J. G., and Paz González, A.: Characterizing anisotropy and
484 heterogeneity of soil surface microtopography using fractal models, *Ecological Modelling*, 182,
485 337–353, <https://doi.org/10.1016/j.ecolmodel.2004.04.012>, 2005.
- 486 Wang, J., Fu, B., Qiu, Y., and Chen, L.: Soil nutrients in relation to land use and landscape position in
487 the semi-arid small catchment on the loess plateau in China, *Journal of Arid Environments*, 48, 537–
488 550, <https://doi.org/10.1006/jare.2000.0763>, 2001.
- 489 Wang, Y., Li, S., Lang, X., Huang, X., and Su, J.: Effects of microtopography on soil fungal
490 community diversity, composition, and assembly in a subtropical monsoon evergreen broadleaf
491 forest of Southwest China, *CATENA*, 211, 106025, <https://doi.org/10.1016/j.catena.2022.106025>,
492 2022.
- 493 Wei, C., Ni, J., Gao, M., Xie, D., and Hasegawa, S.: Anthropogenic pedogenesis of purple rock fragments in



- 494 Sichuan Basin, China, CATENA, 68, 51–58, <https://doi.org/10.1016/j.catena.2006.04.022>, 2006.
- 495 Zheng, J.-J., He, X.-B., Walling, D., Zhang, X.-B., Flanagan, D., and Qi, Y.-Q.: Assessing Soil Erosion
- 496 Rates on Manually-Tilled Hillslopes in the Sichuan Hilly Basin Using ^{137}Cs and $^{210}\text{Pb}_{\text{ex}}$
- 497 Measurements, *Pedosphere*, 17, 273–283, [https://doi.org/10.1016/S1002-0160\(07\)60034-4](https://doi.org/10.1016/S1002-0160(07)60034-4), 2007.
- 498 Zhong, S., Wei, C., Ni, J., Xie, D., and Ni, C.: Characterization of clay rock-derived soils containing
- 499 multi-mineral sand particles in upland areas of Sichuan Basin, China, CATENA, 194, 104737,
- 500 <https://doi.org/10.1016/j.catena.2020.104737>, 2020.